

Sequence-based prediction of the intrinsic solubility of peptides containing non-natural amino acids

Received: 6 March 2023

Accepted: 26 October 2023

Published online: 17 November 2023

 Check for updates

Marc Oeller^{1,6}, Ryan J. D. Kang¹, Hannah L. Bolt², Ana L. Gomes dos Santos³, Annika Langborg Weinmann⁴, Antonios Nikitidis⁵, Pavol Zlatoidsky⁵, Wu Su⁵, Werngard Czechtizky⁵, Leonardo De Maria⁵, Pietro Sormanni¹✉ & Michele Vendruscolo¹✉

Non-natural amino acids are increasingly used as building blocks in the development of peptide-based drugs as they expand the available chemical space to tailor function, half-life and other key properties. However, while the chemical space of modified amino acids (mAAs) such as residues containing post-translational modifications (PTMs) is potentially vast, experimental methods for measuring the developability properties of mAA-containing peptides are expensive and time consuming. To facilitate developability programs through computational methods, we present CamSol-PTM, a method that enables the fast and reliable sequence-based prediction of the intrinsic solubility of mAA-containing peptides in aqueous solution at room temperature. From a computational screening of 50,000 mAA-containing variants of three peptides, we selected five different small-size mAAs for a total number of 37 peptide variants for experimental validation. We demonstrate the accuracy of the predictions by comparing the calculated and experimental solubility values. Our results indicate that the computational screening of mAA-containing peptides can extend by over four orders of magnitude the ability to explore the solubility chemical space of peptides and confirm that our method can accurately assess the solubility of peptides containing mAAs. This method is available as a web server at <https://www-cohsoftware.ch.cam.ac.uk/index.php/camsolptm>.

Peptides are a growing drug market with over 100 approved drugs, with insulin being the most prominent one^{1–3}. Peptide drugs exhibit several advantages over small molecules². Since they often exhibit low toxicity and may not accumulate in tissue, they can be safe while having high efficacy². They are also diverse, potent, easy to synthesise²

and have higher specificity, due to their larger size compared to small molecules⁴. However, peptide drug candidates can suffer from several problems. They tend to have low oral bioavailability and short half-lives^{1,2,5} caused by high clearance rates and low metabolic stability due to the presence of peptidases^{1,2,5}. Moreover, peptides can have poor

¹Centre for Misfolding Diseases, Yusuf Hamied Department of Chemistry, University of Cambridge, Cambridge, UK. ²Hit Discovery, Discovery Sciences, BioPharmaceuticals R&D, AstraZeneca, Cambridge, UK. ³Advanced Drug Delivery, Pharmaceutical Sciences, BioPharmaceuticals R&D, AstraZeneca, Cambridge, United Kingdom. ⁴Early Chemical Development, Pharmaceutical Sciences, BioPharmaceuticals R&D, AstraZeneca, Gothenburg, Sweden. ⁵Medicinal Chemistry, Research and Early Development, Respiratory and Immunology, BioPharmaceuticals R&D, AstraZeneca, Gothenburg, Sweden. ⁶Present address: Proteomics and Signal Transduction, Max Planck Institute of Biochemistry, Martinsried, Germany. ✉ e-mail: ps589@cam.ac.uk; mv245@cam.ac.uk

membrane permeability, tend to aggregate, can contain immunogenic sequences^{2,6}, and their conformational flexibility may generate problems during drug development as they can adopt more than one structure⁵.

Taking example from nature, the properties of endogenous peptides and proteins can be modified through post-translational modifications (PTM)⁷. Typical PTMs include phosphorylation for signal transduction and energy metabolism^{8,9}, and acetylation and glycosylation for regulation¹⁰. Other common modifications are amidation, carboxylation, hydroxylation, disulfide bond formation, sulfation and proteolytic cleavage^{11,12}. PTM dysregulation is often associated with disease, including sleeping sickness¹³, amyloid-associated diseases¹⁴ and HIV¹⁵. A particular focus in recent years has been put on the impact of PTMs on protein aggregation, and on associated neurodegenerative diseases^{6,16}. Different PTMs have been shown to have varying effects on the aggregation propensity of peptides and proteins⁶. N-terminal truncation, incorporation of pyroglutamate, phosphorylation and nitration increases oligomerisation of the amyloid- β peptide, while citrullination and backbone modifications also increase oligomerisation but simultaneously decrease aggregation⁶. In therapeutic applications, examples include the increase in biological activity and improvement of metabolic stability by N-methylation^{17,18}, increasing binding affinity^{4,19}, half-life increase and improvement of tissue penetrating abilities by lipidation and acylation⁶. Methylation can also increase binding selectivity¹⁹.

By adopting strategies that extend the scope of PTMs, the use of modified amino acids (mAAs) has become prominent in biotechnology and drug development³, through a variety of methods to engineer mAAs into proteins^{20–29}. A selection of the most common mAAs is shown in Table 1, with those used in this work being highlighted in bold. General approaches to improve peptide-based drugs often start with alanine or glutamic acid scanning to identify interaction and cleavage sites⁵, and continue with the replacement of natural amino acids with modified amino acids (mAAs) to tailor a variety of other properties^{1,5}. These mAAs can contain new functional groups, and alter the backbone or the terminal structure of a peptide^{5,30}. The effects of mAAs are diverse and can counter specific problems inherent in biologics, including by altering immunogenicity³¹. One of the major issues in peptide drug development is the recognition by proteases and peptidases, which can be attenuated by changing the backbone through incorporation of amide bond mimics, D-isomers, β -amino acids, alteration of the termini or tetra-substituted amino acids^{1,4,17,19,31–36}. These mimics also tend to increase bioavailability, another issue which often plagues peptide drugs¹⁷ as well as restrict conformation and therefore reduce flexibility^{1,37,38}. Similar effects can also be caused by N-alkylations^{1,17}, incorporation of aminoisobutyric acid³⁹, other constraining amino acids^{31,40,41} or by cyclisation^{1,19,36,38}. The latter and addition of sterically bulky groups can also reduce T-cell recognition^{4,19}. Bioavailability and stability can also be improved by glycosylation, which enhances protein-protein interactions and makes use of glucose transporters on the cell surface which improves cell permeability³¹. Permeability can also be improved by increasing hydrophobicity, which can be achieved by methylation, lipidation³¹, and by adding fluorinated residues¹⁹ or modifications to terminal residues⁴².

Many applications based on mAAs have been made in materials science, especially with nanotubes and nanofibres^{43–46}. mAAs can be also used for photoactive, photo- or fluorescent-caged and photocrosslinking modifications^{47–56}, fluorescent probes^{47,48,57–60}, spectroscopic probes^{47,48,61} and as metal ion chelators^{47,48}. Moreover, they can be used to create redox-active enzymes⁶², reduce the complexity of NMR spectra⁶³ and can have antimicrobial activity⁶⁴.

Commercial vendors currently offer hundreds of synthesis-ready mAAs that can be synthesised into peptides and it has been shown recently that this chemical space can be greatly expanded⁶⁵. At the same time, experimental methods to characterise peptides are

Table 1 | Selection of the most common modified amino acids (mAAs)

Amino Acid	Modification
Ala	N-acetylation (N-terminus)
Ala	Aminoisobutyric acid
Ala	Cyclohexylalanine
Ala	Addition of a primary amine
Arg	Deimination to citrulline
Arg	Dimethylation (N, N-Met)
Arg	Methylation (O-Met)
Arg	Methylation (N-Met)
Asn	Deamidation to Asp or iso-Asp
Asn	N-linked glycosylation
Asp	Isomerization to isoaspartic acid
Asp	N-acetylation (N-terminus)
Cys	Disulfide-bond formation
Cys	N-acetylation (N-terminus)
Cys	Oxidation to sulfonic acid
Cys	S-nitrosylation
Gln	Cyclization to pyroglutamic acid (N-terminus)
Gly	N-acetylation (N-terminus)
His	Phosphorylation
Leu	Norleucine
Leu	Methylation (tert-Butyl-Alanine)
Lys	Hydroxylation
Lys	Acetylation
Lys	Methylation
Lys	Ubiquitination
Lys	SUMOylation
Met	N-acetylation (N-terminus)
Met	Oxidation to sulfoxide
Met	Oxidation to sulfone
Phe	C-amidation (C-terminus)
Pro	Hydroxylation
Ser	N-acetylation (N-terminus)
Ser	O-linked glycosylation
Ser	Phosphorylation
Thr	N-acetylation (N-terminus)
Thr	O-linked glycosylation
Thr	Phosphorylation
Trp	Di-oxidation
Trp	Formation of naphthalene
Trp	Mono-oxidation
Tyr	C-amidation (C-terminus)
Tyr	Phosphorylation
Tyr	Sulfation
Val	N-acetylation (N-terminus)

The mAAs used in this work are highlighted in bold.

often material-intensive and time-consuming. State-of-the-art solubility measurements such as PEG solubility assays, require substantial amounts of material, and have a throughput typically unsuitable for the screening of thousands of candidates^{66–69}. Therefore, developing computational methods to predict the intrinsic solubility and aggregation propensity of peptides and proteins with mAAs would be highly beneficial. Laborious solubility measurements could be avoided or greatly reduced by incorporating fast and inexpensive in silico screenings in development pipelines. Although there are

several accurate protein and peptide solubility predictors available as well as predictors for individual amino acids, to our knowledge no sequence-based method can readily handle non-natural amino acids^{70–74}.

To bridge this gap, here we exploited the CamSol framework for the prediction of intrinsic solubility^{75–77} to develop the CamSol-PTM method, which can handle peptides containing mAAs that are of similar size to canonical amino acids. CamSol-PTM is capable of assessing the effect of any kind of small-size noncanonical amino acid on the intrinsic solubility of peptides in aqueous solution at room temperature by combining a range of different physicochemical property predictors. The absolute solubility of a peptide is the combination of its intrinsic solubility and external factors that impact its solubility such as solvents, ionic strength and pH. By focusing on predicting intrinsic solubility, we aim at creating a general model that can be extended to take external factors into account⁷⁷. The base model is focusing on the intrinsic solubility in aqueous solutions at room temperature. We experimentally validate this approach on variants of three peptides incorporating different mAAs at most positions. The wild-type peptides, which we include in the validation, are glucagon-like peptide-1 (GLP-1), tyrosine tyrosine (PYY), and 18 A.

GLP-1 is a peptide used to treat several disorders, most notably obesity and type-2 diabetes^{78–80}. It reduces appetite, glucagon secretion and slows down gastric emptying⁸⁰, and has a low risk of inducing hypoglycemia, a common side effect for diabetes drugs⁷⁸. GLP-1 is a 36 amino acid long peptide that when cleaved at the N-terminus produces its active form: GLP-1_{7–36} amide⁷⁸. The drawback of GLP-1 in its native form is that, like most peptides, it has a short half-life and fast clearance rate⁸⁰. The GLP-1 derivatives liraglutide and semaglutide were developed to overcome this issue^{80,81}. The half-life of these drugs is significantly extended compared to its native form by introducing long fatty acid chains that improves drug half-life primarily by enabling albumin binding^{82–87}.

PYY acts similarly to GLP-1 and is sometimes administered in combination with it to treat obesity, as it is co-released by the body when nutrients are detected⁸¹. In addition to appetite regulation, it affects energy and glucose homeostasis^{81,88,89}. PYY is a gut hormone with a length of 36 amino acids, although its major form is truncated at the N-terminus to give PYY_{3–36}⁸⁸. Other truncated variants such as 1–34 and 3–34 are also present but appear to be inactive⁸¹. The C-terminus of PYY binds four different receptors of the neuropeptide Y receptor family^{81,89}. It has a similarly short half-life as GLP-1, approximately 10 minutes⁸¹.

18 A is a derivative of apolipoprotein A (ApoA-1) which is the major component of high-density lipoproteins (HDLs)². Apolipoproteins are complexes that contain lipids and proteins, which transport lipids and other hydrophobic molecules through the body⁹⁰. HDLs can remove cholesterol by decreasing low-density lipoproteins (LDLs) and therefore act against lipid imbalance which is a major cause for cardiovascular diseases². ApoA-1 is a 243 amino acid-long protein that consists of 10 amphipathic α -helices which interact with lipids². 18 A is an 18 amino acid long peptide⁹¹ that mimics these α -helices². Since the original 18 A design, many improvements were made to increase its affinity to lipids and homology to ApoA-1 such as acetylating the N-terminus and amidating the C-terminus^{2,90}.

For each of these peptides, we screened computationally over 10,000 variants containing combinations of 5 different mAAs. For validation, we then synthesised 30 of those peptides and measured their solubility for the initial set. A second set of 7 peptides containing 4 new mAAs was used to confirm the generalisability of our approach. Our results show that CamSol-PTM can reliably predict the intrinsic solubility of peptides containing mAAs, showing high correlation between predicted and experimentally measured relative solubility.

Results

Computational predictions

In this work we exploited the CamSol framework for the accurate prediction of the intrinsic solubility of proteins^{75–77} to introduce a method able to predict the effect of mAAs on the solubility of peptides. The original CamSol method predicts the intrinsic solubility of proteins by combining tabulated values of hydrophobicity, charge, and α -helical and β -sheet propensities of the 20 standard amino acids. To extend these tables to a range of different mAAs, information on the physicochemical properties of these mAAs is required (Fig. 1). Because our goal is to estimate the intrinsic solubility of mAA-containing peptides without the need to carry out extensive experimental studies, we build a pipeline in which the physicochemical properties of the mAAs are predicted computationally.

pKa values

We calculated pKa values of modified side-chains using the recently developed pIChemist suite which calculates ionisation constants using pKaMatcher⁹². pKaMatcher matches SMARTS patterns of the mAAs with a list of SMARTS patterns with known pKas⁹².

Hydrophobicity

CamSol uses hydrophilicity values closely related to the inverse of experimental logP values⁷⁵. Here, to develop a predictor of the hydrophobicity of the mAAs, we used a combination of different hydrophobicity calculators to reduce possible biases. After considering the results of several benchmarks, we selected three hydrophobicity predictors: ALOGPS, XLOGP3 and KOWWIN^{93–95}. All these methods are machine learning-based, which train their algorithms on different descriptors. ALOGPS^{96,97} is based on creating 75 electrotopological-state (E-state) indices trained on the Physprop database (*Syracuse Research Corporation. Physical/Chemical Property Database (PHYSPROP); SRC Environmental Science Center: Syracuse, NY. (1994)*)^{93,98}. XLOGP3 is an atomic-based model⁹⁹ that uses 87 atomic groups and two correction factors⁹³. KOWWIN is fragment-based, using 150 different fragments and 250 corrections^{93,100}.

Next, we fitted the hydrophobicity values for the 20 natural amino acids as calculated with these predictors to the tabulated CamSol hydrophilicity values. This fit accomplishes two goals. First, the original tabulated values of the 20 natural amino acids do not have to be changed. Second, aligning mAA hydrophilicity values to the original value range bypasses the need to re-fit the parameters used to combine the different biophysical properties in the CamSol framework⁷⁵. We thus calculated the correlation of each of these individual predictors with the original hydrophilicity values of CamSol for the 20 standard amino acids (Supplementary Fig. 1a–c). Using a linear regression analysis, we obtained a fit function to the target values, which showed a higher correlation than with the individual predictors with a Pearson's coefficient of correlation of 0.9 (Supplementary Fig. 1d). Although the combination of the three predictors was accurate, KOWWIN was not suited for the automation of the whole process. Since KOWWIN is only available as part of the EPA suite which only runs on Windows and is not open source, it would be very laborious to include this in the process¹⁰¹. However, we found that the accuracy of CamSol-PTM is not significantly affected when using only the other two predictors (Pearson's coefficient of correlation = 0.88) (Supplementary Fig. 1e).

Secondary structure propensity

We set out to develop a predictor of secondary structure propensity for mAAs based on physico-chemical properties. The values for the 20 standard amino acids are calculated using statistics from the PDB⁷⁵. However, many types of mAAs are either too rare or altogether absent in the PDB, meaning that a new approach was needed. We considered the following characteristics: molecular weight (MW), number of

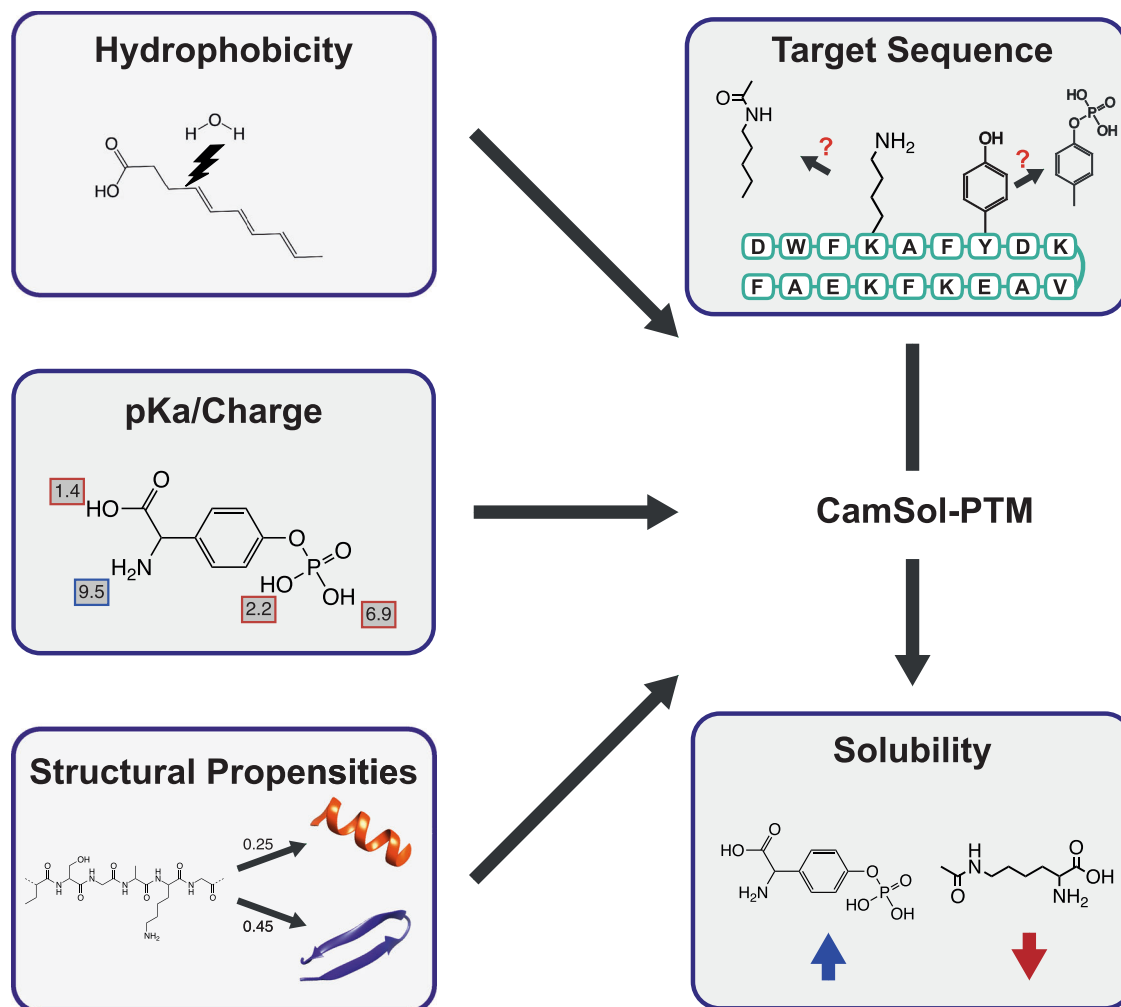


Fig. 1 | Workflow for optimising the solubility of peptides containing modified amino acids (MAAs) using CamSol-PTM. A linear combination of ALOGPS^{96,97} and XLOGP3¹⁰⁰ is employed to determine the hydrophobicity values. pChemSt suite⁹² is used to predict the pKa values of MAAs. Structural propensities are calculated using a separate predictor that gives an estimate on the likelihood of finding a MAA

in an α -helix or a β -sheet. The predictor employs a combination of the number of hydrogen donors and acceptors, the number of rotational bonds, molecular weight and the topological polar surface area. All this information is fed into the CamSol-PTM algorithm to predict the effect of MAAs on the solubility of a peptide.

hydrogen donors (H_D) number of hydrogen acceptors (H_A) number of rotational bonds (RB) and topological polar surface area (TPSA). The information on these properties for all standard amino acids and the MAAs used in this work were initially gathered from <https://pubchem.ncbi.nlm.nih.gov/>. The final version of CamSol calculates these values using the python module RDKit. To determine which combination of properties would yield the best predictor, we explored a series of linear equations for different combinations of these five properties, such for example

$$p_i^\alpha = \alpha_{MW} * MW_i + \alpha_{TPSA} * TPSA_i + \alpha_{RB} * RB_i, \quad (1)$$

where p_i^α is the calculated α -helical propensity of amino acid i and α_x are the linear coefficients to be fitted. For each combination of the properties, we fitted a function to the tabulated secondary structure propensity values of the standard amino acids. We excluded glycine and proline, since these two amino acids have unusual secondary structure propensities and would skew the fit. Moreover, we also used the resulting secondary structure propensity values of each of these combinations within the CamSol-PTM framework to predict the solubilities of all peptides. To choose which secondary structure propensity predictor was the most promising we looked at the Pearson's coefficients of correlation between the predicted secondary

structure propensity values and their tabulated counterparts as well as at the correlation between the experimental and predicted solubility data for the 30 peptide variants. The choice of propensities that offered the best combination of high correlation for the secondary structure propensities as well as the high correlation between the predicted and experimental solubilities while simultaneously using as few parameters as possible was H_D and TPSA for α -helical propensities ($R=0.59$) and MW, RB and TPSA for β -sheet propensities ($R=0.69$, Supplementary Fig. 2).

Sequence parser

As a 1-letter alphabet is not available for all possible MAAs, we parsed the input sequence as follows. MAAs are added to the standard protein sequence as a three-letter code in square brackets (e.g. Ala-norleucine-Gly would be denoted as 'A[NLE]G'). A careful literature research regarding nomenclature for denoting MAAs showed that there is currently no widely used and simultaneously easy-to-read format for coding MAAs. Therefore, we kept the implementation flexible in order for any kind of nomenclature to be used.

Choice of modifications

To decide the set of MAAs for an initial testing, we considered a range of different functionalities. Acetylation of native lysine (NAC) residue is

a common PTM with great impact on the properties of a peptide, as it removes a positive charge. Aminoisobutyric acid (AIB) is often used to make peptides more resistant against peptidases as it is not easily recognised⁷⁹. Norleucine (NLE) is closely related to the natural amino acids leucine, valine and isoleucine, but with its longer non-branched aliphatic chain offers a slightly different functional group; it is also typically used as a non-oxidation labile methionine substitution. Cyclohexylalanine (CHA) offers a unique functionality due to its highly hydrophobic non-aromatic six-membered ring. Citrulline (CIT) offers alternative functionality that resembles arginine. Moreover, we also implemented modifications to the N- and C-termini of peptide scaffolds: N-acetylated aspartic acid, C-amidated phenylalanine and C-amidated tyrosine as these were already included in the base peptides. With this mix of new functionalities and some closely related mAAs we aimed to cover a broad chemical space.

Peptide design

Due to the limit of the number of possible variants that could be synthesised and purified in this study, we wanted to ensure that our designs covered the largest possible chemical space while exploring a broad range of solubility values. For each peptide we designed five variants each containing one mAA. We chose alanine residues as the starting point for single modifications to have a common baseline for all mAAs. Additionally, we screened all possible combinations of double modifications for each peptide. The first step, however, was to define regions for each peptide that allowed for modification without interfering with the binding capabilities and specific folds.

GLP-1 consists of two α -helices separated by a linker. We chose the first alanine in the linker region (residue 24) as the starting point for single-site modifications. For the double-site modifications, we further excluded the following residues due to their essential role in binding: 7His, 8Ala, 9Glu, 11Thr, 12Phe, 13Thr, 14Ser, 16Val, 17Ser, 18Ser, 19Tyr, 20Leu, 21Glu, 26Lys, 28Phe, 29Ile, 31Tyr, 32Leu, 33Val, 34Lys.

PYY consists of a proline-rich α -helix at the N-terminus which forms H-bonds with the α -helix that comprises the rest of the molecule. Hence, we chose an alanine in the proline-rich region to perform the single-site modifications. For the double-site modifications, we excluded all prolines and hydrogen-bonding residues, i.e. R, H, K, D, E, N, Q.

18A has an amphipathic nature that is convenient to maintain. Therefore, for the single-site modifications, we chose alanine at position 10, located on the edge between the two sides. For the double-site modifications, we ensured that the hydrophilic residues (D, E, K) were only replaced with hydrophilic modifications (CIT, AIB) and hydrophobic residues (W, F, A, V) were only replaced with hydrophobic mAAs (CHA, NAC, NLE).

Given these constraints, we screened over 50,000 mAA variants using CamSol-PTM. From all these possible variants for double modifications, we chose at least one variant where one of the modifications is rather small, e.g., L to NLE, F to CHA, A to AIB or R to CIT. For the remaining three doubly modified variants per peptide, we chose one variant each predicted as either very soluble, very insoluble or average in solubility. The sequences of the designed peptides are given in Table 2.

Generation of experimental data

Relative solubility was measured using a recently developed PEG precipitation assay⁶⁶. For all PYY variants the standard assay worked well, and no changes had to be implemented (Fig. 2a). Variants 27 and 28 were completely soluble whereas variant 30 was already insoluble in the absence of PEG, and variant 29 proved to be difficult to produce and purify. Therefore, these four are not reported in Fig. 2. 18A and its variants proved more complicated, as most variants were completely soluble up to 30% PEG. We therefore switched from PEG to ammonium sulphate (AMS) precipitation (Fig. 2b), as it has been shown that relative solubility measurements with PEG and AMS are correlated¹⁰².

Moreover, to ensure that the results stemming from the AMS assay are consistent and reliable, we performed the 18A experiments twice independently on different days. The results confirmed that they are indeed replicable, and we were therefore confident to use them for the validation of our approach (Supplementary Fig. 3). Two variants, namely variant 17 and 18 proved to be completely insoluble and variant 12 was not produced in sufficient amounts. Therefore, these are not reported in the figures. The last set of variants stemming from GLP-1 had the inverse problem, as most variants proved to be very insoluble. Even at final concentrations of 0.33 mg/mL (instead of 1 mg/mL) most variants remained insoluble. We used ultracentrifugation to determine the relative solubilities of the GLP-1 variants (Table 3). To confirm the reliability of this method we replicated the results on a different day with the same stock solutions (Supplementary Fig. 4).

Correlation between predicted and experimental solubility values

By comparing the computational predictions with the experimental data, we found high correlations between the two data sets. The Pearson's coefficients of correlation for the PYY variants are 0.78, 0.81 for the 18A variants and 0.58 for the GLP1 variants (Fig. 3). To ascertain that these findings were not merely a coincidence, we designed a second set of PYY variants containing four new mAAs and measured their solubilities (Fig. 2c). The results are depicted in Fig. 3a in ochre. Variant 32 is not depicted as it was not possible to measure its solubility with the PEG Assay. The overall Pearson's coefficient of correlation for the combined set of PYY variants is 0.6.

Encouraged by the results of the experimental validation, we set out to generalise the computational approach to broaden its applicability to more mAA types. We set up a web server under <https://www-cohsoftware.ch.cam.ac.uk/index.php/camsolptm> for academic user to freely use our method. We automated the process of adding new mAAs by replacing the hydrophobicity predictor with the Crippen tool from RDKit. If a user would like to predict the solubility of a peptide containing a noncanonical amino acid that has not been implemented yet, only the SMILES code is required. By providing this information, the web server will automatically calculate the necessary properties for this mAA in order for the user to include it in the prediction.

To demonstrate the speed of the automation, we incorporated the whole set of non-canonical amino acids that Amarasinghe *et al.* recently produced through extensive *in silico* screenings⁶⁵. CamSol-PTM can calculate about 15 new residues per second on a single CPU core. We then designed 40,000 single mutational variants of a 60 residue-long Nrf2 peptide fragment centred around the mutational sites Leu76, Asp77, Glu78 and Leu84, which were previously identified⁶⁵. We predicted the intrinsic solubility for each of these variants which took 8 min on a single CPU core (around 80/s) and plotted the distribution of the solubilities (Fig. 4). By analysing the tail ends of the distribution, we found that, in agreement with chemical intuition, mAAs that contain many hydrogen bonding residues such as those containing nitrogen and oxygen atoms are among the most solubility-promoting residues (Supplementary Fig. 5). The mAAs that most negatively affected the solubility largely contain several aromatic rings and often halogens such as chlorine or bromine (Supplementary Fig. 6).

Discussion

Peptide intrinsic solubility is one of the most crucial parameters that determine the likelihood of a peptide to be successfully developed into a commercial drug product. Application of automated, predictive technologies with high throughput and low compound requirements are very useful for efficient early profiling and optimization of physico-chemical properties, such as solubility during early discovery program allowing for more comprehensive screenings and faster development times.

Table 2 | List of peptides designed to verify the CamSol-PTM predictions

Compound	Peptide	Sequence	Modifications
1	GLP1	HAEGTFTSDVSSYLEGQAAKEFIAWLVKGR	None
2	GLP1	HAEGTFTSDVSSYLEGQ[CHA]AKEFIAWLVKGR	A -> CHA
3	GLP1	HAEGTFTSDVSSYLEGQ[NLE]AKEFIAWLVKGR	A -> NLE
4	GLP1	HAEGTFTSDVSSYLEGQ[NAC]AKEFIAWLVKGR	A -> NAC
5	GLP1	HAEGTFTSDVSSYLEGQ[AIB]AKEFIAWLVKGR	A -> AIB
6	GLP1	HAEGTFTSDVSSYLEGQ[CIT]AKEFIAWLVKGR	A -> CIT
7	GLP1	HAEGTFTSDVSSYLEGQ[CHA]AKEFIAWLVKGR[CIT]	A -> CHA, R -> CIT
8	GLP1	HAE[AIB]TFTSDVSSYLEGQAAKEF[CIT]AWLVKGR	G -> AIB, I -> CIT
9	GLP1	HAEGTFTS[CHA]VSSYLEGQA[NAC]FIAWLVKGR	D -> CHA, E -> NAC
10	GLP1	HAE[NLE]TFTSDVSSYLEG[CIT]AAKEFIAWLVKGR	G -> NLE, Q -> CIT
11	18 A	[ntDAC]WFKAFYDKVAEKFEA[ctFAD]	None
12	18 A	[ntDAC]WFKAFYDKV[CHA]EKFEA[ctFAD]	A -> CHA
13	18 A	[ntDAC]WFKAFYDKV[NLE]EKFEA[ctFAD]	A -> NLE
14	18 A	[ntDAC]WFKAFYDKV[NAC]EKFEA[ctFAD]	A -> NAC
15	18 A	[ntDAC]WFKAFYDKV[AIB]EKFEA[ctFAD]	A -> AIB
16	18 A	[ntDAC]WFKAFYDKV[CIT]EKFEA[ctFAD]	A -> CIT
17	18 A	[ntDAC]W[CHA]KAFYDKV[CHA]EKFEA[ctFAD]	F -> CHA, A -> CHA
18	18 A	[ntDAC]WFK[CHA]FYDKVAEKFE[NLE][ctFAD]	A -> CHA, A -> NLE
19	18 A	[ntDAC]WF[AIB]AFYDKVAEK[CHA]KEA[ctFAD]	K -> AIB, F -> CHA
20	18 A	[ntDAC]W[NAC]KAFYDKVAEK[NLE]KEA[ctFAD]	F -> NAC, F -> NLE
21	PYY3-36	IKPEAPREDASPEELNRYASLRHYLNLVTRQR[ctYAD]	None
22	PYY3-36	IKPEAPRED[CHA]SPEELNRYASLRHYLNLVTRQR[ctYAD]	A -> CHA
23	PYY3-36	IKPEAPRED[NLE]SPEELNRYASLRHYLNLVTRQR[ctYAD]	A -> NLE
24	PYY3-36	IKPEAPRED[NAC]SPEELNRYASLRHYLNLVTRQR[ctYAD]	A -> NAC
25	PYY3-36	IKPEAPRED[AIB]SPEELNRYASLRHYLNLVTRQR[ctYAD]	A -> AIB
26	PYY3-36	IKPEAPRED[CIT]SPEELNRYASLRHYLNLVTRQR[ctYAD]	A -> CIT
27	PYY3-36	IKPEAPRED[CIT]SPEELNRYASLRHY[NLE]NLVTRQR[ctYAD]	A -> CIT, L -> NLE
28	PYY3-36	IKPEAPRED[NLE]PEELNRYA[NLE]LRHYLNLVTRQR[ctYAD]	S -> NLE, S -> NLE
29	PYY3-36	IKPE[AIB]PREDASPEELNRYA[NAC]LRHYLNLVTRQR[ctYAD]	A -> AIB, S -> NAC
30	PYY3-36	[AIB]KPEAPREDASPEELNRYASLRHYLNL[AIB]TRQR[ctYAD]	I -> AIB, V -> AIB
31	PYY3-36	IKPEAPRED[DAP]SPEELNRYASLRHYLNLVTRQR[ctYAD]	A -> DAP
32	PYY3-36	IKPEAPRED[NAP]SPEELNRYASLRHYLNLVTRQR[ctYAD]	A -> NAP
33	PYY3-36	IKPEAPRED[TBA]SPEELNRYASLRHYLNLVTRQR[ctYAD]	A -> TBA
34	PYY3-36	IKPEAPRED[OPO]SPEELNRYASLRHYLNLVTRQR[ctYAD]	A -> OPO
35	PYY3-36	IKPE[CHA]PREDASPEELNRYASLRH[OPO]LNLVTRQR[ctYAD]	A -> CHA, Y -> OPO
36	PYY3-36	IKPE[OPO]PREDASPEELNRYASLRHYL[TBA]VTRQR[ctYAD]	A -> OPO, L -> TBA
37	PYY3-36	[CIT]KPEAPREDASPEE[AIB]NRYASLRHY[DAP]NLVTRQR[ctYAD]	I -> CIT, L -> AIB, L -> DAP

Initially, for each peptide, nine variants were designed. Five include single-site modifications, one is a double-site modification where one modification is small and three are random double-site modifications. In a second step another seven variants for PYY were designed (31–37) containing four new mAAs.

Non-canonical amino acids are often used to introduce unique functionalities to drugs such as peptidase resistances^{1,4,17,19,31–36} or increase binding affinities^{4,19}. However, experimental methods to evaluate the developability of peptides containing mAAs are typically costly, and current computational approaches lack the capability of capturing the effects of mAAs on the solubility of peptides. To address this problem, we have presented CamSol-PTM, a software that predicts the intrinsic solubility in aqueous solution at room temperature of peptides and proteins containing non-canonical amino acids based on the physicochemical properties of their amino acid sequences^{75–77}.

To test the CamSol-PTM predictions, 30 variants of 3 peptides containing 5 different mAAs were chosen from a preliminary screen of over 50,000 designs. The peptides were produced and purified, and their solubilities were experimentally measured. The comparison between measurements and predictions showed that CamSol-PTM can predict the intrinsic solubility of peptides and proteins containing

mAAs with high accuracy (Pearson's coefficients of correlation 0.72 on average).

We confirmed the generalisability of our approach by designing a second set of PYY variants with four new mAAs and measured their solubility and compared it to our predictions. The high overall Pearson's coefficient of correlation for the whole set of PYY variants – although being slightly lower at 0.6 – showcases the robust applicability of our method.

Although the wild types of the peptides tested in this study tend to form α -helices, we do not expect our method to be significantly biased towards this type of secondary structure. First, most parameters, including the ones to calculate the solubility score for individual amino acids and the parameters used to determine the overall solubility of a protein are identical to original CamSol method which was trained on a wide range of varying secondary structure. Second, the mAAs tested were not merely α -helical promoting residues and are therefore not biased towards α -helical structures.

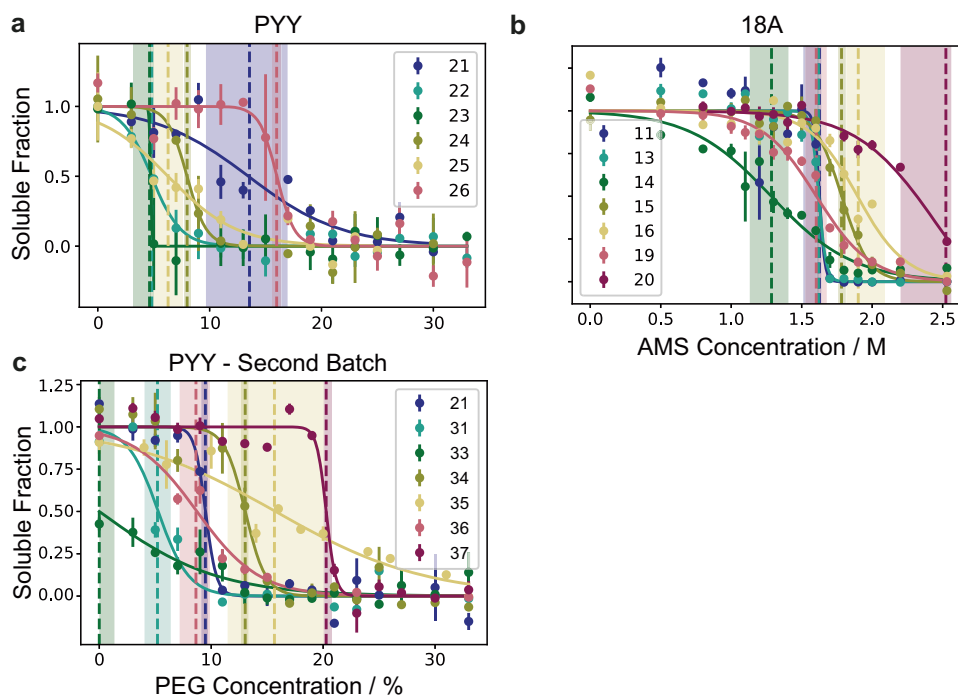


Fig. 2 | Experimental solubility data for peptides generated using the PEG solubility assay. Solubility curves determined using a recently developed PEG solubility assay⁶⁶ for all successfully synthesised variants (all designs except variants 12 and 29) that are neither completely soluble (variants 27 and 28) nor insoluble (variants 17, 18 and 30) for: PYY (a), 18 A (b) and the second batch of PYY variants (c). For 18 A AMS was used instead of PEG. $PEG_{1/2}/AMS_{1/2}$ values are shown

as a vertical line with the shaded region depicting the 95% confidence interval. PEG percentages are mass/volume⁶⁶. Error bars represent the standard error of the experimental measurements across technical replicates ($n = 4$ for PYY and PYY – Second Batch, $n = 2$ for 18 A) where the centre represents the mean. Source data are provided as a Source Data file.

It has been recently shown that by creating new unnatural amino acids in silico, it is possible to create effective new compounds, thus demonstrating the potential of incorporating more diverse mAAs into the drug development process⁶⁵. By automating the process of adding new mAAs to CamSol-PTM, the method is now capable of predicting the effects of small mAAs on the solubility of proteins and peptides. We have demonstrated the speed and versatility of the method by adding all 10,000 mAAs reported recently by Amarasinghe et al. to our method and predicting the solubility of 40,000 mutational variants of a Nrf2 peptide fragment⁶⁵.

We acknowledge that although our method increases the chemical space that can be covered by solubility predictions by several orders of magnitude compared to the 20 natural amino acids, it is currently restricted to modifications that are of similar size to canonical amino acids. Further developments will be required to assess the effects of larger modifications such as lipids or glycans on the intrinsic solubility of peptides.

We envisage that the CamSol-PTM method will substantially aid in the understanding of the effects of non-canonical amino acids on the intrinsic solubility of proteins and peptides. As with previous

versions, it can also be used to identify aggregation hot spots by analysing the solubility profiles. Moreover, we expect it to be a valuable tool for drug development as it enables the fast and accurate solubility prediction of peptides containing modified amino acids.

Methods

Materials

N- α -D-Fmoc protected amino acids were sourced from Bachem AG (Switzerland). Synthesis reagents and solvents were all obtained from NovaBioChem, Merck (UK) and used without further purification. Peptide sequences were prepared using automated microwave-assisted solid phase peptide synthesis using the CEM Liberty Blue synthesiser and Fmoc chemistry with standard side chain protecting groups.

Peptide synthesis

All peptides were synthesised as C-terminal carboxamides on Rink Amide MBHA resin (loading 0.23 mmol/g, 100–200 mesh) on a 0.1 mmol scale using DIC/HOBt activation. All amino acids were double coupled for 4 min at 75 °C, with the instrument set to deliver the N- α -Fmoc-amino acid solutions (0.2 M solution in DMF), HOBt (1.0 M solution in DMF) and DIC (1.0 M solution in DMF). Deprotection cycles were performed using 20% piperidine solution (in DMF, + 0.1 mol HOBt) for 1 min at 90 °C following each cycle. Crude peptides were cleaved from the resin using a cleavage cocktail containing TFA (95%), triisopropylsilane (2.5%) and water (2.5%) for 4 hours at room temperature. The resin was removed by filtration and the cleavage solution removed *in vacuo*. The peptides were precipitated by addition of diethyl ether, isolated by centrifuge at 3500 rpm and dried under a flow of dry nitrogen.

Table 3 | Experimental solubility data for the GLP-1 variants generated using ultracentrifugation

Variant	1	2	3	4	5	6	7	8	9	10
Run 1 / mg/mL	0.58	0	0.09	S	0.09	S	0.84	S	0	0.15
Run 2 / mg/mL	1.38	0	0.16	S	0.07	S	0.82	S	0	0.12

Results of two independent ultracentrifugation runs measuring the solubility of the GLP-1 variants. S symbolizes the outcomes in which no precipitation occurred.

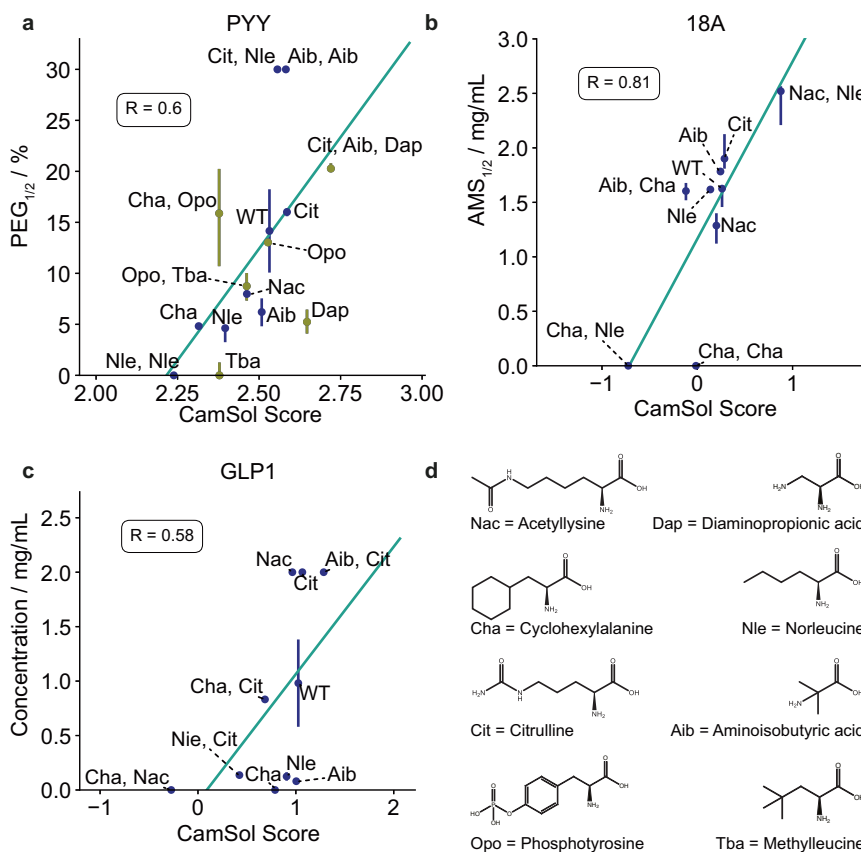


Fig. 3 | Correlation between experimental and predicted solubility values of the designed peptides containing mAAs. The Pearson's coefficients of correlation are 0.6 for PYY (0.78 for the initial set) (a), 0.81 for 18 A (b) and 0.58 for GLP1 (c). mAAs that were used are shown in (d). The two designs (12 and 29) that could not be produced in sufficient amounts were removed from the analysis. Error bars in a and b represent the 95% confident intervals of the $PEG_{1/2}$ values stemming from the

sigmoidal function fitted through the experimental measurements shown in Fig. 2 (technical replicates $n = 4$ for a and $n = 2$ for b) where the centre represents the mean. Error bars in c represent the standard error of the experimental measurement shown in Table 3 across technical replicates ($n = 2$) where the centre represents the mean. Source data are provided as a Source Data file.

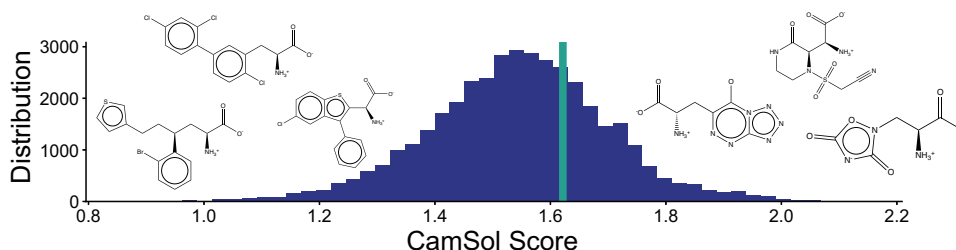


Fig. 4 | Solubility distribution of 40,000 variants of the Nrf2 peptide fragment. Single mutants were designed containing one of the recently reported 10,000 mAAs⁶⁵ at one of four positions (Leu76, Asp77, Glu78, Leu84). Solubility of the wild-type peptide is highlighted with a turquoise line. Analysis of the tail ends of the distribution revealed that mAAs that contain many hydrogen-bonding promoting

atoms such as nitrogen and oxygen are predominantly found in the highly soluble region, whereas mAAs with halogens such as chlorine and bromine and aromatic rings are mostly found in the insoluble region. The vertical line depicts the CamSol score for the wild type Nrf2 peptide fragment. Source data are provided as a Source Data file.

Peptide purification and analysis

Prior to purification, crude peptides were reconstituted in 5% acetonitrile in water (v/v) or dissolved in TFA and diluted with ACN/Water/TFA 50/50/0.1 mixture and filtered (0.4 μ m, PTFE). The purifications were performed by preparative HPLC (Waters Fraction Lynx system connected to a PDA detector and Waters SQD mass spectrometer) using a Waters Atlantis T3 OBD column, Waters XSelect CSH Fluoro Phenyl OBD column or a Waters XBridge C18 OBD column with a focused acetonitrile gradient at room temperature. The mobile phases used were either at acidic or neutral conditions. For specific conditions

see Supplementary Data 1. Fraction collection was triggered on either a UV threshold or target mass intensity threshold, the UV trace was monitored at 230 nm. The collected fractions were pooled and analysed on a C8 or a C18 column by Waters UPLC system (or Agilent 1200 series gradient HPLC system) using a linear acetonitrile gradient at acidic conditions (Supplementary Data 1). UV purity was estimated to between 82 and 99% at 210 nm or 230 nm on a Waters H-Class UPLC system with a PDA, Waters SQD mass spectrometer (or Waters 3100 system). Target masses were verified against theoretical values on the mass spectrometer operating in ES⁺ mode.

Solubility assay

Aliquots of 1 mg were prepared from the purified and lyophilised stocks. The solubility of the PYY and 18 A variants was measured using the PEG solubility assay that was developed in this group⁶⁶. Briefly, a precipitant is titrated in increasing concentration to a fixed concentration of protein to induce precipitation of the protein. The samples are incubated for 48 h at 4° after mixing. The samples are centrifuged and the remaining protein concentration is measured in the supernatant using a plate reader. PYY and 18 A variants were dissolved in 10 mM citrate 10 mM phosphate buffer at pH 7 for a final concentration of 3 mg/mL. The assay was run with 50% 6000 PEG for PYY and with 3.8 M AMS for 18 A. To improve throughput, a multi-channel robot was employed to measure several peptides at once with the workflow being kept the same as described previously⁶⁶. The solubility of the GLP1 variants was measured with ultracentrifugation as follows: The peptides were dissolved in 10 mM citrate 10 mM phosphate buffer at pH 7 for a final concentration of 2 mg/mL. 120 µL of each sample were centrifuged using an OptimaTLX Ultracentrifuge and spinning for 30 min at 500,000 g at 4 °C. The supernatant was removed, and the peptide concentration was measured using a NanoDrop.

Reporting summary

Further information on research design is available in the Nature Portfolio Reporting Summary linked to this article.

Data availability

All peptide sequences are given in Table 2 and Supplementary Data 1. All data necessary to replicate, evaluate or extend the research presented in this article are provided throughout the article, the supporting information and the Source Data file. All predicted values are provided in the Source Data file and can be replicated by using the webserver under <https://www-cohsoftware.ch.cam.ac.uk/index.php/camsolptm>. Information on peptide production and purification are included in the supporting information. Source data are provided with this paper.

Code availability

This method is available as a web server which is free for academic users after registration at <https://www-cohsoftware.ch.cam.ac.uk/index.php/camsolptm>. For industry users it is possible to purchase a license for the CamSol method from Cambridge Enterprise.

References

- Qvit, N., Rubin, S. J. S., Urban, T. J., Mochly-Rosen, D. & Gross, E. R. Peptidomimetic therapeutics: scientific approaches and opportunities. *Drug Discov. Today* **22**, 454–462 (2017).
- Recio, C., Maione, F., Iqbal, A. J., Mascolo, N. & De Feo, V. The potential therapeutic application of peptides and peptidomimetics in cardiovascular disease. *Front. Pharmacol.* **7**, 1–11 (2017).
- D'Aloisio, V., Dognini, P., Hutcheon, G. A. & Coxon, C. R. PepTherDia: database and structural composition analysis of approved peptide therapeutics and diagnostics. *Drug Discov. Today* **26**, 1409–1419 (2021).
- Meister, D., Taimoory, S. M. & Trant, J. F. Unnatural amino acids improve affinity and modulate immunogenicity: Developing peptides to treat MHC type II autoimmune disorders. *Pept. Sci.* **111**, e24058 (2019).
- Vlieghe, P., Lisowski, V., Martinez, J. & Khrestchatsky, M. Synthetic therapeutic peptides: science and market. *Drug Discov. Today* **15**, 40–56 (2010).
- Zapadka, K. L., Becher, F. J., Gomes dos Santos, A. L. & Jackson, S. E. Factors affecting the physical stability (aggregation) of peptide therapeutics. *Interface Focus* **7**, 20170030 (2017).
- Ramazi, S. & Zahiri, J. Post-translational modifications in proteins: Resources, tools and prediction methods. *Database* **2021**, 1–20 (2021).
- Graves, J. D. & Krebs, E. G. Protein Phosphorylation and Signal Transduction. *Pharmacol. Ther.* **82**, 111–121 (1999).
- Xu, Y., Xue, D., Bankhead, A. & Neamati, N. Why All the Fuss about Oxidative Phosphorylation (OXPHOS)? *J. Med. Chem.* **63**, 14276–14307 (2020).
- Reily, C., Stewart, T. J., Renfrow, M. B. & Novak, J. Glycosylation in health and disease. *Nat. Rev. Nephrol.* **15**, 346–366 (2019).
- Walsh, G. & Jefferis, R. Post-translational modifications in the context of therapeutic proteins. *Nat. Biotechnol.* **24**, 1241–1252 (2006).
- Walsh, G. Post-translational modifications of protein biopharmaceuticals. *Drug Discov. Today* **15**, 773–780 (2010).
- Kessler, H. et al. Selective Inhibition of Trypanosomal Triosephosphate Isomerase by a Thiopeptide. *Angew. Chem. Int. Ed. Engl.* **31**, 328–330 (1992).
- Sievers, S. A. et al. Structure-based design of non-natural amino-acid inhibitors of amyloid fibril formation. *Nature* **475**, 96–103 (2011).
- Welch, B. D., VanDemark, A. P., Heroux, A., Hill, C. P. & Kay, M. S. Potent D-peptide inhibitors of HIV-1 entry. *Proc. Natl Acad. Sci. Usa.* **104**, 16828–16833 (2007).
- Martin, L., Latypova, X. & Terro, F. Post-translational modifications of tau protein: Implications for Alzheimer's disease. *Neurochem. Int.* **58**, 458–471 (2011).
- Vagner, J., Qu, H. & Hruby, V. J. Peptidomimetics, a synthetic tool of drug discovery. *Curr. Opin. Chem. Biol.* **12**, 292–296 (2008).
- Chatterjee, J., Gilon, C., Hoffman, A. & Kessler, H. N-methylation of peptides: A new perspective in medicinal chemistry. *Acc. Chem. Res.* **41**, 1331–1342 (2008).
- Blaskovich, M. A. T. Unusual Amino Acids in Medicinal Chemistry. *J. Med. Chem.* **59**, 10807–10836 (2016).
- Wang, L. & Schultz, P. G. Expanding the genetic code. *Angew. Chem. - Int. Ed.* **44**, 34–66 (2004).
- Wang, L., Xie, J. & Schultz, P. G. Expanding the genetic code. *Annu. Rev. Biophys. Biomol. Struct.* **35**, 225–249 (2006).
- Wang, W. et al. Genetically encoding unnatural amino acids for cellular and neuronal studies. *Nat. Neurosci.* **10**, 1063–1072 (2007).
- Wang, Q., Parrish, A. R. & Wang, L. Expanding the Genetic Code for Biological Studies. *Chem. Biol.* **16**, 323–336 (2009).
- Wu, X. & Schultz, P. G. Synthesis at the interface of chemistry and biology. *J. Am. Chem. Soc.* **131**, 12497–12515 (2009).
- Kiick, K. L., Saxon, E., Tirrell, D. A. & Bertozzi, C. R. Incorporation of azides into recombinant proteins for chemoselective modification by the Staudinger ligation. *Proc. Natl Acad. Sci. Usa.* **99**, 19–24 (2002).
- Hendrickson, T. L., De Crécy-Lagard, V. & Schimmel, P. Incorporation of nonnatural amino acids into proteins. *Annu. Rev. Biochem.* **73**, 147–176 (2004).
- Hartman, M. C. T., Josephson, K. & Szostak, J. W. Enzymatic aminoacylation of tRNA with unnatural amino acids. *Proc. Natl Acad. Sci. Usa.* **103**, 4356–4361 (2006).
- Lindstedt, P. R. et al. Enhancement of the Anti-Aggregation Activity of a Molecular Chaperone Using a Rationally Designed Post-Translational Modification. *ACS Cent. Sci.* **5**, 1417–1424 (2019).
- Lindstedt, P. R. et al. Systematic Activity Maturation of a Single-Domain Antibody with Non-canonical Amino Acids through Chemical Mutagenesis. *Cell Chem. Biol.* **28**, 70–77.e5 (2021).
- Laxio Arenas, J., Kaffy, J. & Ongerli, S. Peptides and peptidomimetics as inhibitors of protein-protein interactions involving

- β -sheet secondary structures. *Curr. Opin. Chem. Biol.* **52**, 157–167 (2019).
31. Ding, Y. et al. Impact of non-proteinogenic amino acids in the discovery and development of peptide therapeutics. *Amino Acids* **52**, 1207–1226 (2020).
32. Toniolo, C., Crisma, M., Formaggio, F. & Peggion, C. Control of peptide conformation by the Thorpe-Ingold effect (C α -tetra-substitution). *Biopolym. - Pept. Sci. Sect.* **60**, 396–419 (2001).
33. Toniolo, C., Formaggio, F., Kaptein, B. & Broxterman, Q. B. You are sitting on a gold mine! *Synlett* 1295–1310 <https://doi.org/10.1055/s-2006-941573> (2006).
34. Rezaei Araghi, R., Ryan, J. A., Letai, A. & Keating, A. E. Rapid Optimization of Mcl-1 Inhibitors using Stapled Peptide Libraries Including Non-Natural Side Chains. *ACS Chem. Biol.* **11**, 1238–1244 (2016).
35. Liang, G., Liu, Y., Shi, B., Zhao, J. & Zheng, J. An Index for Characterization of Natural and Non-Natural Amino Acids for Peptidomimetics. *PLoS One* **8**, 1–16 (2013).
36. Guillen Schlippe, Y. V., Hartman, M. C. T., Josephson, K. & Szostak, J. W. In vitro selection of highly modified cyclic peptides that act as tight binding inhibitors. *J. Am. Chem. Soc.* **134**, 10469–10477 (2012).
37. Revilla-López, G. et al. Integrating the intrinsic conformational preferences of noncoded α -amino acids modified at the peptide bond into the noncoded amino acids database. *Proteins Struct. Funct. Bioinforma.* **79**, 1841–1852 (2011).
38. Rogers, J. M. & Suga, H. Discovering functional, non-proteinogenic amino acid containing, peptides using genetic code reprogramming. *Org. Biomol. Chem.* **13**, 9353–9363 (2015).
39. Venkatraman, J., Shankaramma, S. C. & Balaram, P. Design of folded peptides. *Chem. Rev.* **101**, 3131–3152 (2001).
40. Zanuy, D., Jiménez, A. I., Cativiela, C., Nussinov, R. & Alemán, C. Use of constrained synthetic amino acids in β -Helix proteins for conformational control. *J. Phys. Chem. B* **111**, 3236–3242 (2007).
41. Zanuy, D. et al. Protein segments with conformationally restricted amino acids can control supramolecular organization at the nanoscale. *J. Chem. Inf. Model.* **49**, 1623–1629 (2009).
42. Oliva, R. et al. Exploring the role of unnatural amino acids in antimicrobial peptides. *Sci. Rep.* **8**, 1–16 (2018).
43. Behanna, H. A., Donners, J. J. J. M., Gordon, A. C. & Stupp, S. I. Coassembly of amphiphiles with opposite peptide polarities into nanofibers. *J. Am. Chem. Soc.* **127**, 1193–1200 (2005).
44. Crisma, M., Toniolo, C., Royo, S., Jiménez, A. I. & Cativiela, C. A helical, aromatic, peptide nanotube. *Org. Lett.* **8**, 6091–6094 (2006).
45. Yang, Z., Liang, G., Ma, M., Gao, Y. & Xu, B. In vitro and in vivo enzymatic formation of supramolecular hydrogels based on self-assembled nanofibers of a β -amino acid derivative. *Small* **3**, 558–562 (2007).
46. Cejas, M. A. et al. Thrombogenic collagen-mimetic peptides: Self-assembly of triple helix-based fibrils driven by hydrophobic interactions. *Proc. Natl Acad. Sci. Usa.* **105**, 8513–8518 (2008).
47. Young, T. S. & Schultz, P. G. Beyond the canonical 20 amino acids: Expanding the genetic lexicon. *J. Biol. Chem.* **285**, 11039–11044 (2010).
48. Liu, C. C. & Schultz, P. G. Adding new chemistries to the genetic code. *Annu. Rev. Biochem.* **79**, 413–444 (2010).
49. Kessler, B. et al. T cell recognition of hapten: Anatomy of T cell receptor binding of a H-2K(d)-associated photoreactive peptide derivative. *J. Biol. Chem.* **274**, 3622–3631 (1999).
50. Lemke, E. A., Summerer, D., Geierstanger, B. H., Brittain, S. M. & Schultz, P. G. Control of protein phosphorylation with a genetically encoded photocaged amino acid. *Nat. Chem. Biol.* **3**, 769–772 (2007).
51. Ai, H. W., Shen, W., Sagi, A., Chen, P. R. & Schultz, P. G. Probing Protein-Protein Interactions with a Genetically Encoded Photocrosslinking Amino Acid. *ChemBioChem* **12**, 1854–1857 (2011).
52. Hino, N. et al. Protein photo-cross-linking in mammalian cells by site-specific incorporation of a photoreactive amino acid. *Nat. Methods* **2**, 201–206 (2005).
53. Bose, M., Groff, D., Xie, J., Brustad, E. & Schultz, P. G. The incorporation of a photoisomerizable amino acid into proteins in *E. coli*. *J. Am. Chem. Soc.* **128**, 388–389 (2006).
54. Wildemann, D. et al. A nearly isosteric photosensitive amide-backbone substitution allows enzyme activity switching in ribonuclease S. *J. Am. Chem. Soc.* **129**, 4910–4918 (2007).
55. Rothman, D. M., Vázquez, M. E., Vogel, E. M. & Imperiali, B. General method for the synthesis of caged phosphopeptides: Tools for the exploration of signal transduction pathways. *Org. Lett.* **4**, 2865–2868 (2002).
56. Vázquez, M. E., Nitz, M., Stehn, J., Yaffe, M. B. & Imperiali, B. Fluorescent caged phosphoserine peptides as probes to investigate phosphorylation-dependent protein associations. *J. Am. Chem. Soc.* **125**, 10150–10151 (2003).
57. Wang, J., Xie, J. & Schultz, P. G. A genetically encoded fluorescent amino acid. *J. Am. Chem. Soc.* **128**, 8738–8739 (2006).
58. Murakami, H., Hohsaka, T., Ashizuka, Y., Hashimoto, K. & Sisido, M. Site-directed incorporation of fluorescent nonnatural amino acids into streptavidin for highly sensitive detection of biotin. *Biomacromolecules* **1**, 118–125 (2000).
59. Summerer, D. et al. A genetically encoded fluorescent amino acid. *Proc. Natl Acad. Sci. Usa.* **103**, 9785–9789 (2006).
60. Hyun, S. L., Guo, J., Lemke, E. A., Dimla, R. D. & Schultz, P. G. Genetic incorporation of a small, environmentally sensitive, fluorescent probe into proteins in *Saccharomyces cerevisiae*. *J. Am. Chem. Soc.* **131**, 12921–12923 (2009).
61. Reid, P. J., Loftus, C. & Beeson, C. C. Evaluating the potential of fluorinated tyrosines as spectroscopic probes of local protein environments: A UV resonance Raman study. *Biochemistry* **42**, 2441–2448 (2003).
62. Shinohara, H., Kusaka, T., Yokota, E., Monden, R. & Sisido, M. Electron transfer between redox enzymes and electrodes through the artificial redox proteins and its application for biosensors. *Sens. Actuators, B Chem.* **65**, 144–146 (2000).
63. Cellitti, S. E. et al. In vivo incorporation of unnatural amino acids to probe structure, dynamics, and ligand binding in a large protein by nuclear magnetic resonance spectroscopy. *J. Am. Chem. Soc.* **130**, 9268–9281 (2008).
64. Karstad, R., Isaksen, G., Brandsdal, B. O., Svendsen, J. S. & Svenson, J. Unnatural amino acid side chains as S1, S1, and S2 probes yield cationic antimicrobial peptides with stability toward chymotryptic degradation. *J. Med. Chem.* **53**, 5558–5566 (2010).
65. Amarasinghe, K. N. et al. Virtual Screening Expands the Non-Natural Amino Acid Palette for Peptide Optimization. *J. Chem. Inf. Model.* 2999–3007 <https://doi.org/10.1021/acs.jcim.2c00193> (2022).
66. Oeller, M., Sormanni, P. & Vendruscolo, M. An open-source automated PEG precipitation assay to measure the relative solubility of proteins with low material requirement. *Sci. Rep.* **11**, 1–10 (2021).
67. Toprani, V. M. et al. A Micro-Polyethylene Glycol Precipitation Assay as a Relative Solubility Screening Tool for Monoclonal Antibody Design and. *Formula. Dev. J. Pharm. Sci.* **105**, 2319–2327 (2016).
68. Gibson, T. J. et al. Application of a high-throughput screening procedure with PEG-induced precipitation to compare relative protein solubility during formulation development with IgG1. *Monoclon. Antibodies. J. Pharm. Sci.* **100**, 1009–1021 (2011).

69. Chai, Q., Shih, J., Weldon, C., Phan, S. & Jones, B. E. Development of a high-throughput solubility screening assay for use in antibody discovery. *MAbs* **11**, 747–756 (2019).
70. Yang, Y., Niroula, A., Shen, B. & Vihinen, M. PON-Sol: Prediction of effects of amino acid substitutions on protein solubility. *Bioinformatics* **32**, 2032–2034 (2016).
71. Lauer, T. M. et al. Developability index: A rapid in silico tool for the screening of antibody aggregation propensity. *J. Pharm. Sci.* **101**, 102–115 (2012).
72. Smialowski, P., Doose, G., Torkler, P., Kaufmann, S. & Frishman, D. PROSO II - A new method for protein solubility prediction. *FEBS J.* **279**, 2192–2200 (2012).
73. Fernandez-Escamilla, A. M., Rousseau, F., Schymkowitz, J. & Serrano, L. Prediction of sequence-dependent and mutational effects on the aggregation of peptides and proteins. *Nat. Biotechnol.* **22**, 1302–1306 (2004).
74. Do, H. T. et al. Melting properties of amino acids and their solubility in water. *RSC Adv.* **10**, 44205–44215 (2020).
75. Sormanni, P., Aprile, F. A. & Vendruscolo, M. The CamSol method of rational design of protein mutants with enhanced solubility. *J. Mol. Biol.* **427**, 478–490 (2015).
76. Sormanni, P., Amery, L., Ekizoglou, S., Vendruscolo, M. & Popovic, B. Rapid and accurate in silico solubility screening of a monoclonal antibody library. *Sci. Rep.* **7**, 8200 (2017).
77. Oeller, M. et al. Sequence-based prediction of pH-dependent protein solubility using CamSol. *Brief. Bioinform.* 1–7 [bbad004](https://doi.org/10.1093/bib/bbad004) <https://doi.org/10.1093/bib/bbad004> (2023).
78. Knudsen, L. B. Inventing Liraglutide, a Glucagon-Like Peptide-1 Analogue, for the Treatment of Diabetes and Obesity. *ACS Pharmacol. Transl. Sci.* **2**, 468–484 (2019).
79. Lau, J. et al. Discovery of the Once-Weekly Glucagon-Like Peptide-1 (GLP-1) Analogue Semaglutide. *J. Med. Chem.* **58**, 7370–7380 (2015).
80. Frederiksen, T. M. et al. Oligomerization of a Glucagon-like Peptide 1 Analog: Bridging Experiment and Simulations. *Biophys. J.* **109**, 1202–1213 (2015).
81. Østergaard, S. et al. The effect of fatty diacid acylation of human PYY3-36 on Y2 receptor potency and half-life in minipigs. *Sci. Rep.* **11**, 1–15 (2021).
82. Pyzik, M., Rath, T., Lencer, W. I., Baker, K. & Blumberg, R. S. FcRn: The Architect Behind the Immune and Nonimmune Functions of IgG and Albumin. *J. Immunol.* **194**, 4595–4603 (2015).
83. Bukrinski, J. T. et al. Glucagon-like Peptide 1 Conjugated to Recombinant Human Serum Albumin Variants with Modified Neonatal Fc Receptor Binding Properties. Impact on Molecular Structure and Half-Life. *Biochemistry* **56**, 4860–4870 (2017).
84. Seijsing, J. et al. An engineered affibody molecule with pH-dependent binding to FcRn mediates extended circulatory half-life of a fusion protein. *Proc. Natl Acad. Sci. USA.* **111**, 17110–17115 (2014).
85. Ryberg, L. A. et al. Solution structures of long-acting insulin analogues and their complexes with albumin. *Acta Crystallogr. Sect. D. Struct. Biol.* **75**, 272–282 (2019).
86. Oganessian, V. et al. Structural insights into neonatal Fc receptor-based recycling mechanisms. *J. Biol. Chem.* **289**, 7812–7824 (2014).
87. Knudsen Sand, K. M. et al. Unraveling the interaction between FcRn and albumin: Opportunities for design of albumin-based therapeutics. *Front. Immunol.* **6**, 1–21 (2015).
88. Manning, S. & Batterham, R. L. The role of gut hormone peptide YY in energy and glucose homeostasis: Twelve years on. *Annu. Rev. Physiol.* **76**, 585–608 (2014).
89. Xu, B. et al. Elucidation of the binding mode of the carboxy-terminal region of peptide YY to the human Y2 receptor. *Mol. Pharmacol.* **93**, 323–334 (2018).
90. Mishra, V. K. et al. Association of a model class A (apolipoprotein) amphipathic α helical peptide with lipid: High resolution NMR studies of peptide-lipid discoidal complexes. *J. Biol. Chem.* **281**, 6511–6519 (2006).
91. Anantharamaiah, G. M. et al. Studies of synthetic peptide analogs of the amphipathic helix. Structure of complexes with dimyristoyl phosphatidylcholine. *J. Biol. Chem.* **260**, 10248–10255 (1985).
92. Frolov, A. I., Chankeshwara, S. V., Abdulkarim, Z. & Ghiandoni, G. M. pIChemist — Free Tool for the Calculation of Isoelectric Points of Modified Peptides. *J. Chem. Inf. Model.* **63**, 187–196 (2023).
93. Olguin, C. J. M., Sampaio, S. C. & dos Reis, R. R. Statistical equivalence of prediction models of the soil sorption coefficient obtained using different log P algorithms. *Chemosphere* **184**, 498–504 (2017).
94. dos Reis, R. R., Sampaio, S. C. & De Melo, E. B. The effect of different logP algorithms on the modeling of the soil sorption coefficient of nonionic pesticides. *Water Res.* **47**, 5751–5759 (2013).
95. Wu, K., Zhao, Z., Wang, R. & Wei, G. W. TopP-S: Persistent homology-based multi-task deep neural networks for simultaneous predictions of partition coefficient and aqueous solubility. *J. Comput. Chem.* **39**, 1444–1454 (2018).
96. Tetko, I. V., Tanchuk, V. Y., Kasheva, T. N. & Villa, A. E. P. Estimation of Aqueous Solubility of Chemical Compounds Using E-State Indices. *J. Chem. Inf. Comput. Sci.* **41**, 1488–1493 (2001).
97. Tetko, I. V., Tanchuk, V. Y. & Villa, A. E. P. Prediction of n-Octanol/Water Partition Coefficients from PHYSPROP Database Using Artificial Neural Networks and E-State Indices. *J. Chem. Inf. Comput. Sci.* **41**, 1407–1421 (2001).
98. Kier, L. B. & Hall, L. H. An Electrotopological-State Index for Atoms in Molecules. *Pharm. Res.* **7**, 801–807 (1990).
99. Cheng, T. et al. Computation of octanol-water partition coefficients by guiding an additive model with knowledge. *J. Chem. Inf. Model.* **47**, 2140–2148 (2007).
100. Meylan, W. M. & Howard, P. H. Atom/Fragment Contribution Method for Estimating Octanol–Water. *Partit. Coeff. J. Pharm. Sci.* **84**, 83–92 (1995).
101. US EPA. Estimation Programs Interface Suite for Microsoft Windows v 4.11. United States Environmental Protection Agency Washington, DC, USA (2018).
102. Kramer, R. M., Shende, V. R., Motl, N., Pace, C. N. & Scholtz, J. M. Toward a molecular understanding of protein solubility: Increased negative surface charge correlates with increased solubility. *Biophys. J.* **102**, 1907–1915 (2012).

Acknowledgements

M.O. is a PhD student funded by AstraZeneca. P.S. is a Royal Society University Research Fellow (URF/R1/201461). The project was supported by the Wellcome Trust (203249/Z/16/Z).

Author contributions

M.O. and R.J.D.K. performed experiments and M.O. carried out data analysis. H.L.B., A.N., P.Z. and W.S. synthesize the peptide variants and H.L.B. and A.L.W. purified and analysed them. M.O. and P.S. wrote the software. M.O., P.S. and M.V. wrote the original draft of the manuscript. H.L.B., A.L.G.d.S., L.D.M., W.S., A.L.W. and W.C. edited the manuscript. M.O., P.S., A.L.G.d.S., W.C., L.D.M. and M.V. conceived and A.L.G.d.S., L.D.M., P.S. and M.V. supervised the project.

Competing interests

The authors declare the following competing financial interest(s): H.L.B., A.L.G.d.S., A.L., A.N., P.Z., W.S., L.D.M. and W.C. are employees of AstraZeneca and may own stocks or stock options. The remaining authors declare no competing interests.

Additional information

Supplementary information The online version contains supplementary material available at <https://doi.org/10.1038/s41467-023-42940-w>.

Correspondence and requests for materials should be addressed to Pietro Sormanni or Michele Vendruscolo.

Peer review information *Nature Communications* thanks the anonymous, reviewers for their contribution to the peer review of this work. A peer review file is available.

Reprints and permissions information is available at <http://www.nature.com/reprints>

Publisher's note Springer Nature remains neutral with regard to jurisdictional claims in published maps and institutional affiliations.

Open Access This article is licensed under a Creative Commons Attribution 4.0 International License, which permits use, sharing, adaptation, distribution and reproduction in any medium or format, as long as you give appropriate credit to the original author(s) and the source, provide a link to the Creative Commons license, and indicate if changes were made. The images or other third party material in this article are included in the article's Creative Commons license, unless indicated otherwise in a credit line to the material. If material is not included in the article's Creative Commons license and your intended use is not permitted by statutory regulation or exceeds the permitted use, you will need to obtain permission directly from the copyright holder. To view a copy of this license, visit <http://creativecommons.org/licenses/by/4.0/>.

© The Author(s) 2023